

MICROANALYTICAL CHARACTERIZATION OF NORTH DAKOTA FLY ASH

S.A. Benson, D.K. Rindt, G.G. Montgomery, and D.R. Sears

Grand Forks Energy Technology Center
U.S. Department of Energy
Grand Forks, N.D. 58202

INTRODUCTION

Goals of particulate research at the Grand Forks Energy Technology Center (GFETC) include detailed characterization of fly ash with respect to those properties which relate to controlability as well as possible environmental hazards of emissions. The focus is entirely on low-rank western and Gulf Province coals, whose properties are distinctly different from those of eastern coals. Typically the western coals have high moisture, low sulfur, and large variations in the distribution of inorganic constituents.

Beulah, a North Dakota lignite, was used in the combustion tests of primary interest to this paper. This lignite is extraordinarily variable in its inorganic constituents. For example, the sodium content can have a tenfold variation within a few hundred meters in a single seam (1). The specific Beulah lignite used was selected for its high sodium content.

The fly ash was generated for this research using the GFETC Particulate Test Combuster (PTC), illustrated in the schematic in Figure 1. This unit is an axially-fired pulverized coal combustor with a nominal consumption of 34 kg coal/hr. The unit is designed to generate ash characteristic of that produced with similar fuel in a full-sized utility boiler. Axial firing maximizes the fly ash/(bottom ash + slag) ratio. The fly ash samples for analysis were collected at the inlet to the baghouse with two devices, a five-stage multicyclone and a source assessment sampling system (SASS). The flues are equipped with heat exchangers permitting delivery of flue gas to the chosen control device at temperatures from $\sim 100^\circ$ to 390°C . During these tests, the PTC was equipped with an experimental baghouse because of on-going fabric filter research at GFETC. The PTC instrumentation permits measurement of flue gas condition such as temperature and concentrations of SO_2 , NO_x , O_2 , and CO_2 .

The coal and fly ash were characterized by several analytical techniques. The inorganics of the coal were examined by an extraction technique which selectively removes the inorganics depending upon their association in the coal (2). Low temperature ashing with subsequent x-ray diffraction was used to identify the mineral phases of the coal. The fly ash was examined and analyzed by scanning electron microscope/microprobe, Electron Spectroscopy for Chemical Analysis (ESCA), x-ray diffraction and x-ray fluorescence.

COAL CHARACTERISTICS

The inorganics associated with the Beulah lignite consist of a complex mixture of cations bound to the humic acid groups, possible chelates or coordination complexes, minerals formed during coalification, and minerals accumulated during deposition. Traditional and non-traditional methods were used to examine the coal characteristics. The traditional analysis of the lignite is summarized in Table 1 which lists the ultimate analysis, moisture, heating value, and major element ash analysis.

One of the two "non-traditional methods" used is low-temperature ashing in an oxygen plasma at 150°C with x-ray diffraction analysis to determine the crystalline

phases in the ash. The phases identified include SiO_2 (quartz), FeS_2 (pyrite), kaolinite, and CaCO_3 (calcite). The second method involves a procedure which selectively removes inorganics (2). The ion-exchangeable cations and soluble salts are removed with 1M ammonium acetate. The coal is then extracted with 1M hydrochloric acid to remove chelated species, acid decomposable minerals such as carbonates, and oxides. The inorganics remaining in the coal can include FeS_2 , organically bound sulfur, quartz, and clay minerals. The elements found to be extracted with ammonium acetate are Na (100% of the total Na content), Mg (88%), Ca (41%), and K (57%). The elements removed by HCl are Mg (20%), Al (61%), Ca (50%) and Fe (30%). The elements which remain are Si (100%), Fe (70%), Al (40%), and S (100%). Table 2 summarizes a study of the inorganic constituents in Beulah lignite and the geologic formation it is found in.

TABLE 1. TYPICAL COAL AND COAL ASH ANALYSIS OF BEULAH, N.D. LIGNITE

<u>Ultimate Analysis, as Fired</u>		<u>Coal Ash Analysis, Percent</u>	
Carbon	46.29%	SiO_2	22.3
Hydrogen	5.29	Al_2O_3	11.7
Nitrogen	.62	Fe_2O_3	9.8
Sulfur	.99	TiO_2	0.9
Ash	8.2	CaO	15.7
Moisture	27.2	MgO	5.3
Heating value	17,460 J/g	Na_2O	9.9
(7512 Btu/lb)		K_2O	0.7
		SO_3	23.0

ASH SAMPLING

Fly ash is sampled isokinetically in three ways in the PTC: 1) Using a modified U.S. EPA "method 5" (3) dust loading filters; 2) by collection in a Southern Research Institute* 5-stage multicyclone which simultaneously samples isokinetically and size fractionates the ash (4,5); 3) by collection in a three-stage cyclone module of an Acurex* Source Assessment sampling system or "SASS-Train" (6,7). Nominal aerodynamic size ranges for the multicyclone and the SASS-Train, at the stated flow rates, appear in Table 3. Nominal size ranges, expressed as aerodynamic diameters in μm are those corresponding to actual flow rates employed. The figures represent the mass median diameters (D_{50}) or "cut points", of the size distribution entering or leaving the stage.

University of Washington Mark III* cascade impactors were used to more precisely determine particle size distribution (7). The cumulative particle size distribution, expressed in aerodynamic diameters, appears in Figure 2. This data is used only for comparison. The bulk of the characterization work was done on the multicyclone and SASS Train samples because the masses of particles collected by the impactor are very small and inadequate for analysis.

*Reference to specific brand names and models is done to facilitate understanding and neither constitutes nor implies endorsement by the Department of Energy.

TABLE 2. INORGANIC CONSTITUENTS IN BEULAH LIGNITE AND SENTINEL BUTTE FORMATION (2)

Constituent	Beulah Lignite		Sentinel Butte Formation		
	Whole Coal	Sink Fraction	Overburden	Lignite	Underclay
Alkali feldspars	XXX		XX	X	X
Augite				X	
Barute	X			X	
Biotite	X		X		
Calcite/dolomite	X	XX	XX	X	
Chlorite			XX	X	X
Galena	X				
Gypsum		XX		XXX	
Hematite		X		XX	
Hornblende			X		
Illite	XXX		XX	X	X
Kaolinite	XXX	X	XX	XXX	XXX
Magnetite	X				
Montmorillonite			XXX	X	XXX
Muscovite	X				
Plagioclase		X	XXX	X	X
Pyrite	XXX	XXX		XX	
Quartz	XXX	XXX	XXX	XXX	XXX
Rutile	X				
Volcanic glass			X		

XXX Abundant
 XX Common
 X Minor

TABLE 3. AERODYNAMIC SIZE RANGES (UPPER AND LOWER D₅₀ CUT POINTS) AND SAMPLE FLOW RATES OF GFETC'S ASH SAMPLING EQUIPMENT

Instrument	Southern Research Institute Multicyclone					Acurex/Aerotherm SASS Train*		
	1	2	3	4	5	1	2	3
Flow rate employed STD l/min	9.36					113.2		
Stage No.	1	2	3	4	5	1	2	3
Nominal size range (upper and lower D ₅₀), μm	>10.3	10.3-5.6	5.6-4.15	4.15-1.9	1.9-1.55	>10	10-3	3-1

RESULTS AND DISCUSSION

Fly ash samples were collected by the SASS Train to provide larger masses but only 3 size cuts for x-ray fluorescence (XRF) and x-ray diffractions (XRD). The

elemental trends determined by XRF analysis show increasing concentration of Na_2O and SO_3 and decreasing SiO_2 , CaO , Fe_2O_3 , and MgO with decreasing particle size. Very little change was noted for Al_2O_3 or the minor elements (TiO_2 , K_2O , and P_2O_5). These relationships are illustrated graphically in Figure 3. X-ray diffraction was used to identify the crystalline species in each size fraction. The trends show the following relationships.

1. Na_2SO_4 , $\text{Na}_2\text{Ca}(\text{SO}_4)_2$ are present in the smaller size fractions.
2. SiO_2 , CaO noted in larger size fractions and not in smaller size fractions. Fe_3O_4 - MgFe_2O_4 - MgO phases decrease from larger to smaller size fractions.
3. Possible Al_2SiO_5 and K_2SO_4 phases noted in smallest size fractions.

These two bulk particle characterization methods show the trends of the elemental distribution versus particle size and how the elements are combined. The most interesting trend is the increasing amount of Na_2O and SO_3 with decreasing particle sizes. This leads to the particle-to-particle characterization using the scanning electron microscope/microprobe for various sizes of particles collected with the 5-stage multicyclone.

The scanning electron microscope (SEM) equipped with an energy dispersive x-ray analyzer was used to image and analyze particles down to $\sim 1\mu\text{m}$ in size. The particles were selected at random for analysis by using a grid overlay of points generated by random numbers on the SEM photomicrograph. A typical SEM photomicrograph is shown in Figure 4. One hundred particles for each stage were analyzed, determining 10 elements per particle, and sized. All data was entered into a computing system for correlation analysis.

The average particle size determined from the SEM photomicrographs for each stage are listed in Table 4. Table 4 also lists the Na_2O and SO_3 concentration averages for all five stages along with the ratio of Na_2O to SO_3 . The concentrations of Na_2O and SO_3 increase as particle decreases and the ratio of Na_2O to SO_3 is very close to that of pure Na_2SO_4 for stages 1, 3, and 4. The particles collected in stage 5 are not consistent with the other stages in particle-size or in the ratio of Na_2O to SO_3 . The reason for the inconsistency in the ratio could be due to the bimodal distribution of SO_3 shown in Figure 5, and also to the presence of $\text{Na}_2\text{Ca}(\text{SO}_4)_2$ noted by XRD in the small size fraction of the SASS samples.

The compositional relationships can be represented by plots of composition versus composition for selected constituent pairs. These plots can be used to ascertain the origin of certain species from the original mineral matter of the coal and the interactions that have occurred during combustion. For example, Figure 6 illustrates the compositional plots for several combinations. Figure 6-1 represents the plot of Al_2O_3 versus SiO_2 which reveals a cluster of points around a slope of approximately 0.8. Minerals having been identified in Beulah (2) include biotite, kaolinite, muscovite, and illite, where the Al/Si ratio is in the range of 0.67-1.0. From this it can be suggested that the aluminosilicate framework remains intact after combustion. The common clay minerals have a range in composition of 25-45% Al_2O_3 and 35-50% SiO_2 . Since most of the particles in Figure 6-1 contain less than these percentages, either the aluminosilicates somehow became combined with additional elements or became coated.

The plot of Na_2O versus CaO in Figure 6-2 shows inverse relationship which is supported by the XRF data in Figure 3.

In the plots of SiO_2 versus SO_3 and Al_2O_3 versus SO_3 , Figures 6-3 and 6-4, there is a crude negative correlation between SiO_2 or Al_2O_3 and SO_3 . Despite considerable scatter, many of the points lie in the region along lines connecting clay minerals, at 0% SO_3 , with Na_2SO_4 or glauberite at 0% SiO_2 . This is consistent with clay-like particles becoming coated with Na_2SO_4 .

TABLE 4. SIZE, SODIUM, AND SULFUR RELATIONSHIPS
FOR EACH STAGE OF THE MULTICYCLONE

Stage	Weight Average			
	Particle Size, μm	Na_2O , %	SO_3 , %	$\text{Na}_2\text{O}/\text{SO}_3$
1	5.48	8.60	10.98	0.79
2	1.99	10.78	12.53	0.86
3	1.29	13.20	17.02	0.78
4	1.20	13.98	19.43	0.72
5	1.38	14.99	23.05	0.65

$\text{Na}_2\text{O}/\text{SO}_3$ in pure $\text{Na}_2\text{SO}_4 = 0.78$

Surface analysis of the particles was performed utilizing ESCA. The ESCA analysis technique analyzes to a depth of 20 to 30Å. A typical ESCA scan is shown in Figure 7 for Stage 5 particles. The major constituents found on the surface include Ba, O, Ca, Na, C, S, and Si. The published binding energies (8) of the elements detected by the detailed ESCA scans show that Na, Ca, and Ba are present as sulfates. The Na, Al, and Si may be tied up as silicates, but detailed binding energies for such compounds are unavailable in the literature.

The surfaces of the particles were characterized by a sputter-etching technique used to remove surface layers followed by subsequent ESCA analysis. It was found that carbon and sulfur were concentrated on the surface of all five stages of the multicyclone samples. Contamination of the surface of the particles can largely be attributed to the high concentration of carbon. The presence of sodium was noted on the surface of the larger particles but in the smaller size fractions ($<1.5 \mu\text{m}$) the sodium concentration was more uniform throughout the depth analyzed by sputtering. Campbell and others (9) also showed that Na, S, and C were found on the surface of ash particles. In all cases, except for Stage 5, Ca, Al, and Si were found to increase after sputtering.

CONCLUSIONS

The most significant trend noted by all techniques was the increase of sodium and sulfur with decreasing particle size. The relatively more volatile sodium salts may sublime to form very small particles of pure salt or they may condense on the surfaces of other particles such as aluminosilicates originating from clay minerals of the coal. The latter is supported by the results of the SEM data in Figures 6-3 and 6-4 and the ESCA results. These results support the validity of vaporization-condensation mechanisms of particulate formation. A summary of the possible mechanisms of particulate formation are described by Damle and others (10).

The work described here is part of an ongoing project at GFETC to develop a model for ash formation during the combustion of low-rank coals.

ACKNOWLEDGMENTS

The authors would like to thank Robin Roaldson for his assistance in analyzing particles with the scanning electron microscope and Harold Schobert for his helpful comments in preparation of this paper.

REFERENCES

1. S.A. Cooley, R.C. Ellman, "Analysis of the Northern Grest Plains Province lignites and subbituminous coals and their ash", U.S. Dept. of Energy DOE/ GFETC/ RO-81/2, July 1981.
2. H.H. Schobert, S.A. Benson, M.L. Jones, and F.R. Karner, "Studies in the characterization of United States low-rank coals", Proceedings, International Conference on Coal Science, Dusseldorf, Sept 1981, p.10-15.
3. "Method 5-determination of particle emission from stationary sources", Code of Federal Regulators, Title 40 Part 60, Appendix A, July 1, 1979 pp 143.
4. W.B. Smith, R.R. Wilson, Jr., and R.B. Harris, "A five stage cyclone system for in situ sampling", Environmental Science and Technology, 13, 1387, (1979).
5. W.O. Lipscomb, "Survey of particulate emissions macro- and micro-sampling and sizing methods and real-time monitoring and sizing methods", U.S. Department of Energy, DOE/FC/10193-T1, February, 1981.
6. D.E. Blake, "Source Assessment Sampling System: Design and Development", U.S. Environmental Protection Agency EPA-600/7-78-018, February, 1978.
7. W.B. Smith, P.R. Cavanaugh, and R.R. Wilson, Technical Manual: A Survey of equipment and methods for particulate sampling in industrial process streams. U.S. Environmental Protection Agency, Research Triangle Park, N.C. EPA-600/7-78-043 March, 1978.
8. Handbook of X-ray photoelectron spectroscopy, Perkin-Elmer Corporation, Physical Electronic Division. 1979.
9. J.A. Campbell, R.D. Smith, L.E. Davis, and K.L. Smith, "Characterization of micron-sized flyash particles by X-ray Photoelectron Spectroscopy (ESCA)," The Science of the Total Environment", 12, 75-85, (1979)
10. A.S. Damle, D.S. Ensor, and M.B. Ranade, "Coal combustion aerosol formation mechanisms: A Review", Aerosol Science and Technology 1, 119-133 (1982).

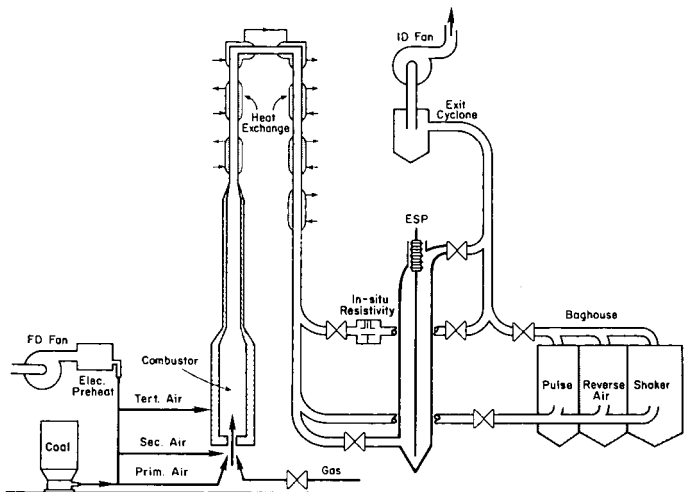


Figure 1. 34 kg/hr Coal Combustion Unit Employed for Ash Generation

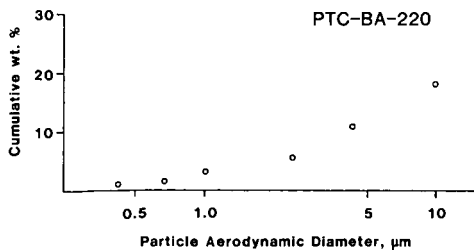


Figure 2. Baghouse Inlet Particle Size Distribution Determined with University of Washington's Mark III Cascade Impactor

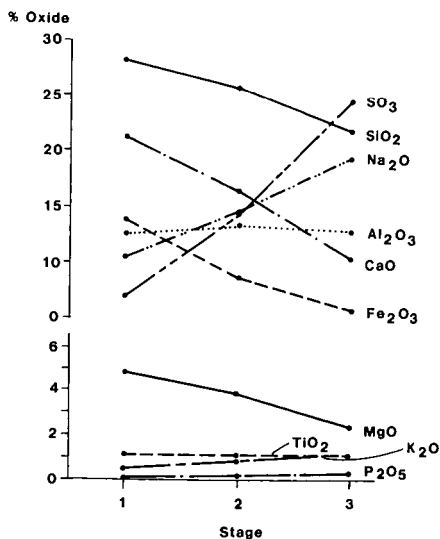


Figure 3. X-ray Fluorescence Analysis of Each Stage from the SASS Train Sampler

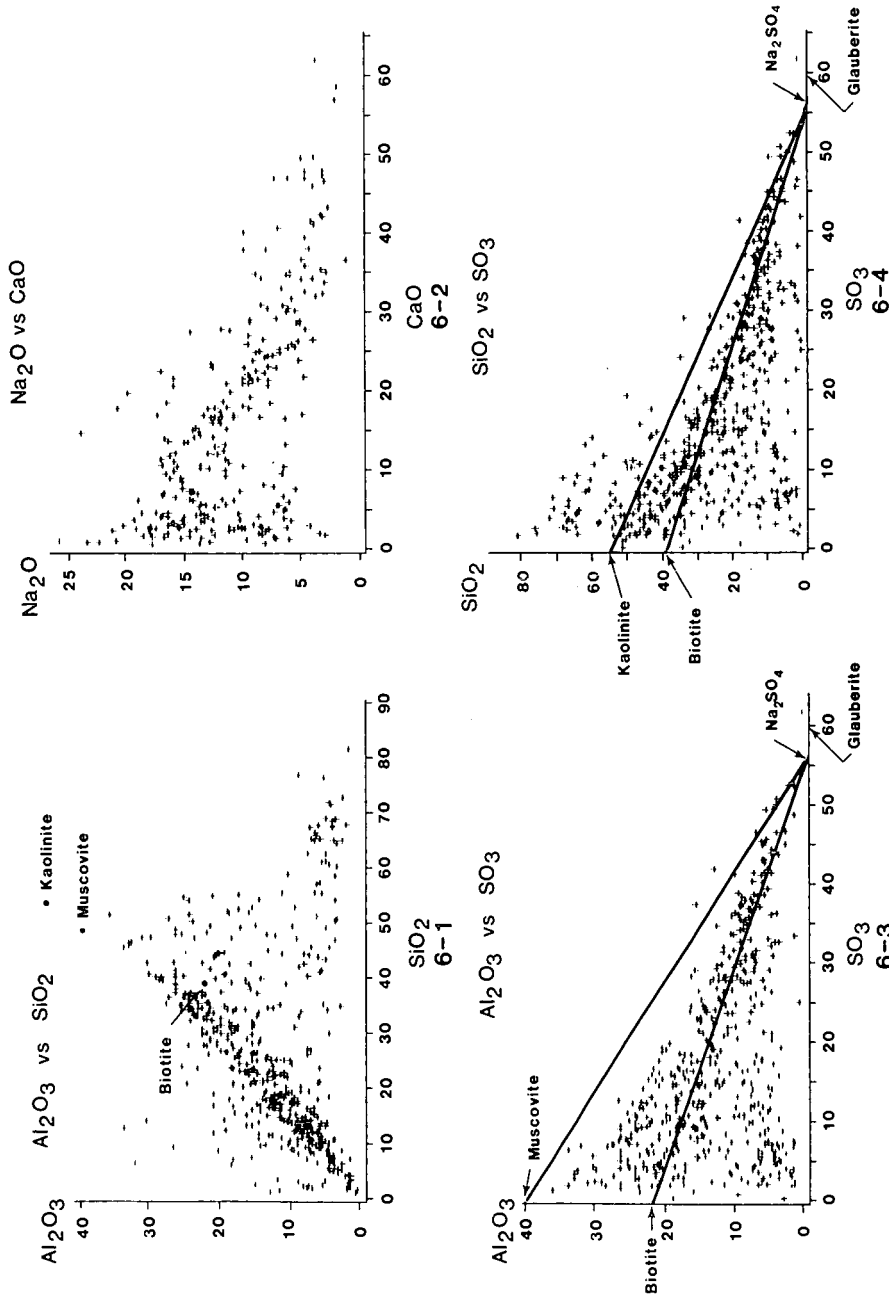


Figure 6. Compositional Relationships for SEM Data Combined from All Five Stages of the Multicyclone

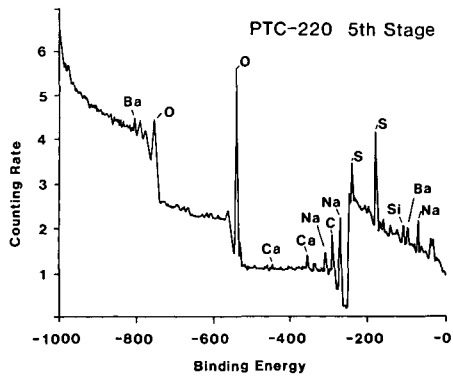


Figure 7. ESCA Scan of Stage 5 of the Multicyclone

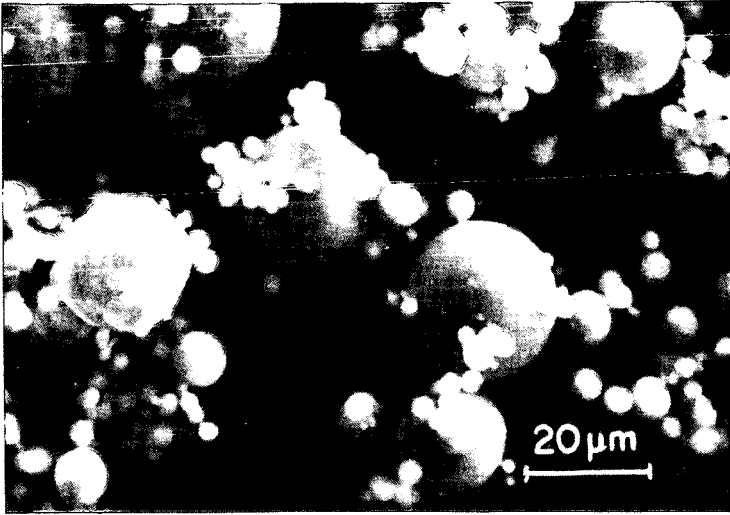


Figure 4. Secondary Electron Image of Particles from Stage 1 Multicyclone

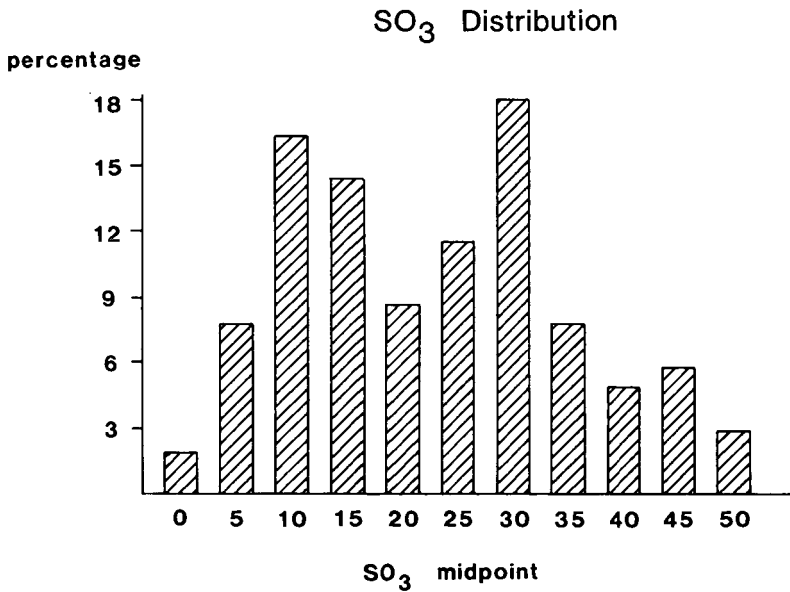


Figure 5. Concentration Population Distribution for SO₃ in Particles Collected in Stage 5 of the Multicyclone